Steel beam–column connection using copper-based shape memory alloy dampers

José Sepúlveda[a], Rubén Boroschek[b], Ricardo Herrera[b], Ofelia Moroni[b,*], Mauricio Sarrazin[b]

[a] *Magna Chile Ltda. Latorre 2077, Calama, Chile*
[b] *Department of Civil Engineering, University of Chile, Blanco Encalada 2002, Piso 4, 837-0449 Santiago, Chile*

Abstract

This study presents the details of an experimental investigation on a prototype partially restrained connection using copper-based shape memory alloy (SMA) bars. The proposed configuration consists of an end-plate connection between a rectangular hollow structural steel beam and a wide flange steel column, where four CuAlBe ($\phi = 3$ mm) bars, in austenitic phase, are used to prestress the end-plate to the column flange. A physical model of the connection was tested by applying a controlled cyclic displacement history at the tip of the beam with two different characteristic frequencies of 0.25 and 1 Hz. Potentiometers and load cells were used to measure strains and stresses in the bars and the displacement and load applied at the beam tip. Similar bars, with the same thermal treatment, had been previously tested in cyclic tension at several nominal strains and frequencies, showing superelastic behavior for deformations up to 2.3% strain. In static tensile tests, the fracture strain was approximately 8%, with a transgranular fracture mechanism. The equivalent damping ratio for the single bar test increases for larger strains, being 6% for a 2.3% strain. The beam–column connection also exhibited superelastic behavior, a moderate level of energy dissipation, and no strength degradation after being subjected to several cycles up to 3% drift. Finally, a set of numerical simulations are conducted to compare the performance of a rigid steel frame and a partially restrained frame with SMA connections using a three-story benchmark structure.
c

Keywords: Shape memory alloys; Beam–column connection; Dampers

1. Introduction

The unexpected damage on steel structures observed after Northridge (1994) and Kobe (1995) earthquakes motivated the development of multiple research projects to investigate and propose solutions to the problems detected. One of the largest research efforts was conducted by a joint venture formed by the Structural Engineers Association of California (SEAOC), the Applied Technology Council (ATC) and the Consortium of Universities for Research in Earthquake Engineering (CUREE). Known as the SAC steel project, this six-year (1994–2000), several million dollar program had the goal of investigating the damage to welded steel moment-frame buildings during the 1994 Northridge earthquake and developing repair techniques and new design approaches to minimize damage to this type of structures in future earthquakes. The project produced a series of technical reports and guidelines for the identification, evaluation, repair, and modification of damaged welded steel moment-frame buildings. Effort was also devoted to new design and construction approaches, culminating in the publication of the FEMA 350 report "Recommended Seismic Design Criteria for New Steel Moment-Frame Buildings" [11], parts of which were later adopted by the American Institute of Steel Construction in its Seismic Provisions [1]. One of the main conclusions from the SAC project was the need to constrain the damage to specific locations where sufficient ductility could be ensured.

Bruneau et al. [3] presented a review of selected research on US seismic design and retrofit strategies for steel structures that include beam-to-column connections, frame modifications at beams' mid-span, self-centering systems, zipper frames, steel plate shear walls, plastic and rotation limits for buildings, and shear links and truss piers for bridges. All these systems and

* Corresponding author. Tel.: +562 9784372; fax: +562 6892833.
E-mail addresses: rborosch@ing.uchile.cl (R. Boroschek), riherrer@ing.uchile.cl (R. Herrera), mmoroni@ing.uchile.cl (O. Moroni), sarrazin@ing.uchile.cl (M. Sarrazin).

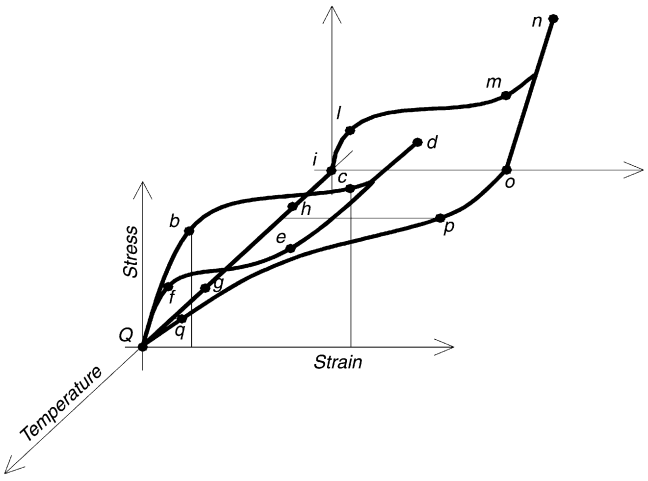

Fig. 1. Typical quasistatic thermomechanical uniaxial response of a SMA element [2].

retrofitting strategies seek to enhance the energy dissipation capacity of structures.

One way of limiting the damage in the main structural members is the use of innovative devices that add damping to the structure and concentrate the inelastic deformations on regions especially detailed to sustain them. These devices may be active (adjust their action according to the response of the structure) or passive (action is the same regardless of the response of the structure). The latter can be divided, according to the damping mechanism, into viscous (e.g. shock absorbers), viscoelastic (e.g. high-damping rubber braces), hysteretic (e.g. yielding steel or lead devices), and superelastic or shape memory alloy (SMA) dampers.

1.1. Shape memory alloys

Shape memory alloys (SMAs) are an extraordinary class of metals that exhibit several unique properties such as large deformation recovery upon heating (shape memory effect) or unloading (superelasticity), high strength, substantial fatigue resistance, and a high level of damping. Among these properties, the superelastic effect of selected SMAs makes them well-suited for passive vibration control techniques. The SMA owes its peculiar characteristics to the transformations between its stable two phases, namely martensite and austenite. Material in the austenite state ("high temperature" phase) transforms to the martensite state ("low temperature" phase) when it is loaded above a certain stress level. Upon unloading the martensite is no longer stable and a reverse transformation to austenite occurs, resulting in complete shape recovery and a substantial hysteretic loop (see Fig. 1).

Four temperatures characterize the phase transformations of SMAs. M_s and M_f indicate the temperatures at which the transformation from austenite into martensite respectively starts and finishes. A_s and A_f indicate the temperatures where the reverse transformation starts and finishes, respectively.

The cyclic behavior of SMAs depends on the type of alloy; the thermomechanical processing (which influences the grain size); the ratio of operating temperature to the phase transformation temperatures; the size of the sample; and the loading history and loading rate. The influence of several of these factors on Ni–Ti elements was studied by Dolce and Cardone [8,9]. More recently, DesRoches et al. [7] found that Ni–Ti wires show higher strength and damping than rods of the same material and that increased loading rates lead to a decrease in equivalent damping.

Aging temperature and aging time are two other factors that influence the behavior of the CuAlBe alloy and its phase transformation temperatures. Flores-Zúñiga et al. [12] measured the martensite start temperature, M_s, for various aging times ranging from 5 min to 500 h (at 250 °C), observing a change in M_s from –42° to –15 °C, respectively.

Thorough reviews concerning potential uses of Ni–Ti-based SMAs in earthquake engineering can be found in DesRoches and Smith [6], Wilson and Wesolowsky [19] and Song et al. [17]. They include state-of-the-art information about modeling, design and testing of devices as well as theoretical and laboratory studies on their use in buildings and bridges.

As part of the MANSIDE and ECOEST II projects, funded by the European Commission, Cardone et al. [4] and Dolce et al. [10] studied the feasibility of using devices with Ni–Ti wires as bracing elements in reinforced concrete structures. A 1:4 scale model of a four-story reinforced concrete 3D frame, with two bays in the longitudinal direction and one bay in the transverse direction was subjected to a series of shake-table tests using a ground motion record from the 1997 Umbría Marche earthquake. The study intended to determine the effectiveness of adding damping to the structure, using two types of dampers (hysteretic and SMA). The parameters of the study included the eccentricity of the structure's mass, and the type of excitation (unidirectional vs. bidirectional ground motion). The structural response was evaluated through the evolution of natural frequencies, equivalent damping ratios, and peak roof displacements of the structure. The experimental results confirmed the effectiveness of using dampers in limiting the damage on the main structural elements.

With respect to Copper-based SMAs, most of the literature covers material science aspects, material models, and mechanical behavior of tertiary alloys such as CuZnAl, CuAlNi and CuAlBe. Studies on the mechanical properties and energy dissipation capacity of Copper-based alloys have been conducted by Witting and Cozzarelli [20] and Gillet et al. [13]. More recently, Casciati and Faravelli [5] and Torra et al. [18] studied the application of a CuAlBe alloy in passive control devices. The CuAlBe alloy is the only Copper-based alloy showing superelastic behavior at room temperature in tension-only cyclic tests that is currently available in the world market.

Previous research on connections incorporating SMA dissipating elements includes a few experimental studies on applications to steel structures. Ocel et al. [14] tested a PR steel beam–column connection using martensite Ni–Ti SMA tendons under cyclic loading. The beam rotation was forced to develop about the center of a shear tab, thereby subjecting the tendons to tension and compression. At 3% drift, severe buckling of the tendons in compression was observed. After heating the tendons, the residual beam tip displacement was

recovered and the connection was re-tested showing repeatable and stable behavior with significant energy dissipation.

SMA elements are a viable alternative when additional energy dissipation is required. One example is a precast concrete connection reported by Priestley [16]. For this connection, the beam is maintained in place by the compression force of an unbonded post-tensioned tendon located at its centerline. Additional structural bars are located at extreme vertical faces of the beam. Moment demands are resisted by the central tendon and by the perimeter bars. Shear is resisted by the frictional force at the beam–column interface provided by the post-tensioning. Energy dissipation capacity is provided only by the structural rebars that are partially unbonded and designed to have a stable yield. However, the residual deformation accumulated in the rebars leads to their buckling, thereby limiting the energy dissipation capacity of the connection. Replacing the yielding bars by superelastic Shape Memory Alloy bars would eliminate the cause of buckling, providing the connection with a significantly larger energy dissipation capacity.

There is, therefore, a need to explore new applications for Copper-based SMA alloys to seismic resistant design. This study evaluates the feasibility of using copper-based shape memory alloy bars on a partially restrained (PR) connection. The proposed configuration consists of an end-plate connection between a rectangular hollow structural steel beam and a wide flange steel column, where four CuAlBe ($\phi = 3$ mm) bars, in austenitic phase, are used to prestress the end-plate to the column flange.

The study involved testing a physical model of the connection, by applying controlled cyclic displacement histories at the tip of the beam with two different characteristic frequencies of 0.25 and 1 Hz. Isolated rods similar to those used in the connection were tested previously under cyclic tension to characterize the mechanical and energy dissipation properties of these components.

Finally, a preliminary investigation about the dynamic effect of the connection in a three-story frame under realistic earthquake motions is performed.

2. Testing of individual SMA bars

The nominal composition of the SMA material used for this study was Cu-11.8% wtAl-0.5% wtBe with $A_f = -2$ °C and $M_s = -16$ °C. Through optical spectroscopy a composition of Cu-10.9% wtAl-0.6% wtBe was obtained. A thermal treatment for 3 min at 850 °C followed by water quenching and immersion in boiling water for 120 min was applied to all bars. The resulting average grain size was about 0.5 mm.

Two types of tests were conducted on 3 mm diameter bars made of the CuAlBe alloy, using a universal testing machine. First, a monotonic quasistatic tension rupture test was performed on a 70 mm long bar. A 25 mm gage length extensometer was used to measure the axial strain in the bar. Rupture occurred at a deformation of 8% and a load of 3.42 kN, corresponding to an equivalent stress of 503.8 MPa, Fig. 2. These values were similar to those obtained by Casciati et al. [5]

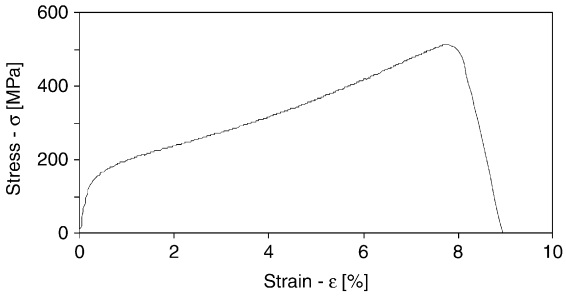

Fig. 2. Force deformation curves for SMA bars.

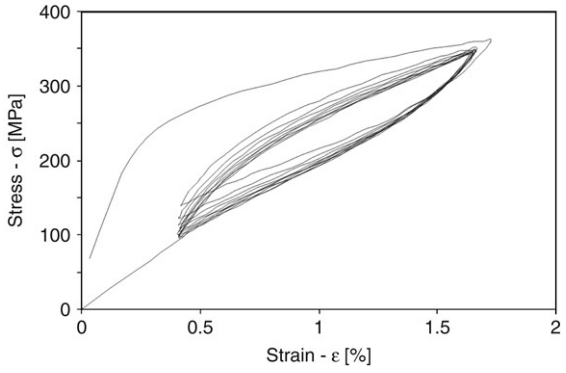

Fig. 3. "Training" effect on individual bars.

for the same material. No sign of bar section reduction could be observed at the fracture zone. The initial elastic modulus E was estimated as 69.74 GPa, and forward transformation started at a stress σ_l equal to 169.4 MPa, corresponding to strain equal to 0.24%.

Second, similar bars were subjected to ten cycles of tension loading–unloading with increasing nominal strain, at ambient temperature. This test was performed at 0.25 and 1 Hz cycling frequency. To avoid inducing compression to the bars a minimum prestrain was used.

A significant stiffening effect was observed in the first cycle for each level of deformation. This effect disappeared for subsequent cycles at deformation amplitudes less or equal than the first cycle, but it appeared again for larger-amplitude cycles. Fig. 3 shows the difference between the first cycle and ten subsequent stable cycles of a bar tested up to 1.72%. This phenomenon, known as "training", has been also reported by previous authors [9].

Fig. 4 shows the response of a bar tested cyclically at 1 Hz. Despite the large number of cycles applied the response is stable, with no significant degradation of load, stiffness, or energy dissipation capacity. In this case the forward transformation stress σ_l was around 250 MPa and the residual strain at the end of the test was less than 0.35%. The ambient temperature during this test was 18 °C.

The secant stiffness, K, the energy density loss per cycle, A_c, and equivalent damping ratio, β, were computed from the hysteretic loops for each test. K was calculated as the difference between the maximum and minimum cyclic stresses divided by the difference between the maximum and minimum cyclic strains. Fig. 5 shows the results of secant stiffness for

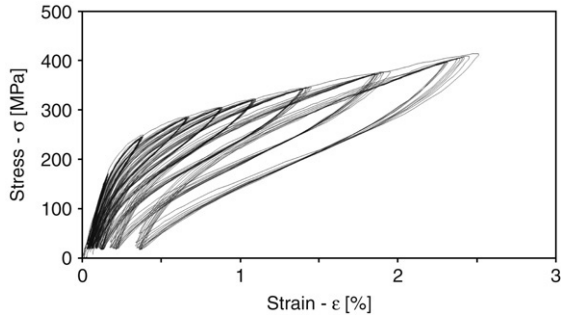

Fig. 4. Single bar force deformation curve for SMA bar, 1 Hz cycling frequency.

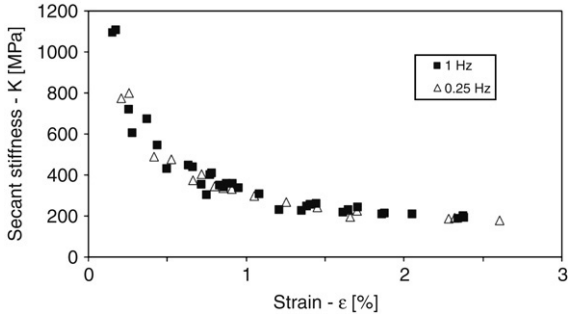

Fig. 5. Rod's secant stiffness.

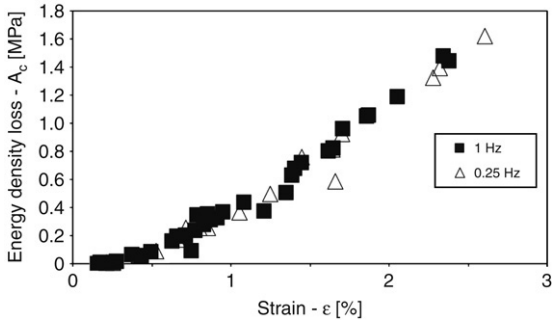

Fig. 6. Single bar dissipated energy as a function of strain.

all the SMA bars tested. It can be seen from this figure that K diminishes with increasing deformations. The energy density loss per cycle, or energy loss per unit volume, was calculated as the area enclosed by the stress–strain hysteresis curve. It can be seen from Fig. 6 that the energy density loss per cycle increases with increasing strain. The equivalent damping ratio was calculated as the (Cycle Area * 100) divided by (2π * Area under the cycle loading curve). This parameter shows a larger dispersion than the secant stiffness (see Fig. 7). In general, the equivalent damping ratio seems to approach a constant value as the deformations get larger.

3. Connection tests

A simple connection test was used to explore the potential of SMA prestressed bars as beam–column joint energy dissipation devices. The model is not a scaled model of a real joint, but it allows evaluation of basic response characteristics.

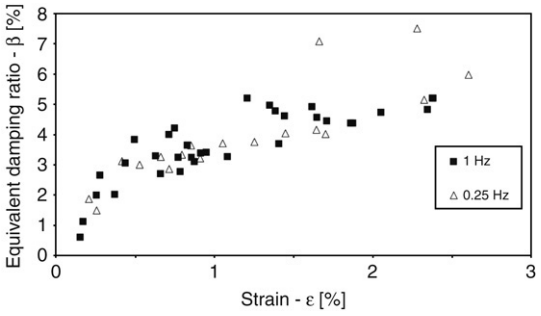

Fig. 7. Equivalent damping ratio for individual bars.

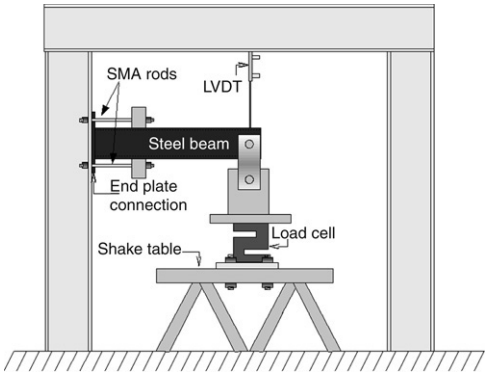

Fig. 8. Experimental setup.

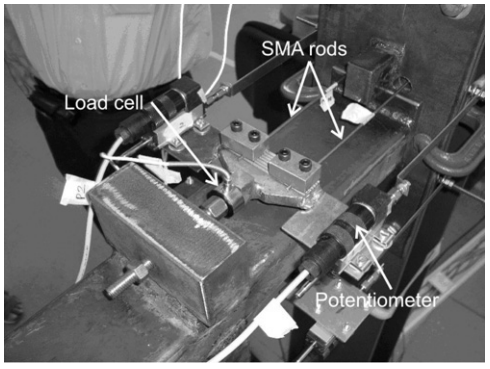

Fig. 9. Detail of SMA clamping and measurement system.

3.1. Experimental test setup

The test specimen consisted of a rectangular hollow structural steel beam (100 × 50 × 4 mm) connected to a wide flange column (150 × 160 × 7 × 9 mm), as shown in Fig. 8. Four 240 mm long, 3 mm diameter SMA bars were fixed into anchorages specially designed to allow for prestressing of the bars, so that they would sustain tension loads only, leaving an effective flexible length of 182 mm, as shown in Fig. 9. This was done to avoid the buckling of the bars under load reversals that was observed in Ocel et al. [14] tests. The beam end-plate was fitted between two steel stubs welded to the flange column above and below the plate. These stubs simplified the erection process and served as stoppers, should the shear on the connection exceed the frictional force between the end-plate and the column flange. At the other end, the beam was pin-connected to a shake table, which was used as an actuator

Table 1
Parameters for connection tests

Test	Frequency (Hz)	Drift (%)	Pre-load at top rods (N)	Pre-load at bottom rods (N)
1	0.25	0.375–1	1465	1449
2	0.25	0.375–1	1996	2018
3	0.25	0.375–1	2400	1600
4	0.25	0.375–1	2040	2030
5	0.25	1.5–2	1997	2020
6	1	0.375–1	2130	1680
7	1	1.5–2	1980	1980
8	0.25	0.375–3	1978	2002
9	0.25	0.375–3	1985	2012
10	0.25	0.375–3	2000	2000

to impose the displacements at the beam tip. The rods were prestressed at the beginning of each test.

3.2. Loading and instrumentation

Four potentiometers were used to measure the displacements in the bars. In addition, an extensometer similar to the one used in the isolated bar tests was attached to one of the rods. Due to test constraints, only two load cells could be used to measure the force on the bars, one for the top rods and the other for the bottom rods, making it impossible to know exactly the load in a single bar. Considering the characteristics of the prestressing mechanism, it was assumed that each rod carried half of the force measured by the corresponding load cell. A potentiometer and a load cell were used to measure the displacement and load at the tip of the beam.

Controlled cyclic vertical displacements were applied at the tip of the beam using the shake table. The loading protocol followed for the test was similar to the SAC steel project protocol, with the intermediate low-amplitude fatigue cycles omitted. The deformation parameter used to determine the loading history was the drift, defined as the beam tip deflection divided by the beam span (970 mm). The connection was tested cyclically at increasing deformation amplitudes ranging from 0.375% to 3% at 0.25 and 1 Hz. Table 1 shows the series of test performed and the prestressing applied to the rods. The ambient temperature during testing was 30 °C.

3.3. Test results

Fig. 10 shows the moment at the connection versus the rotation, measured as the beam tip displacement divided by the beam length, and Fig. 11 shows the forces on the bars versus the rotation considering the top and bottom rods for a test performed at 0.25 Hz. Loops are stable and symmetric.

Due to the shape of hysteresis loop the secant stiffness of the system changes considerably with deformation. Fig. 12 presents this variation indicating that an increase of 10 times the rotation amplitude depresses the secant stiffness to approximately 20% of its original value. The inverse trend is observed for the equivalent damping ratio where the increase with rotations is nearly linear, Fig. 13. For this assembly and for a drift of 3% the damping ratio was approximately

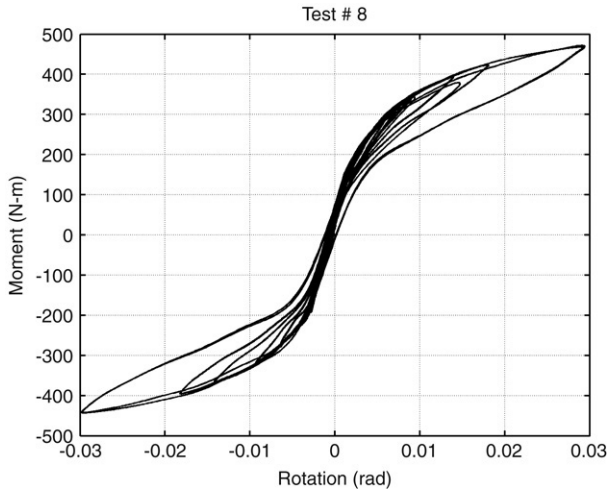

Fig. 10. Moment–rotation of assembly.

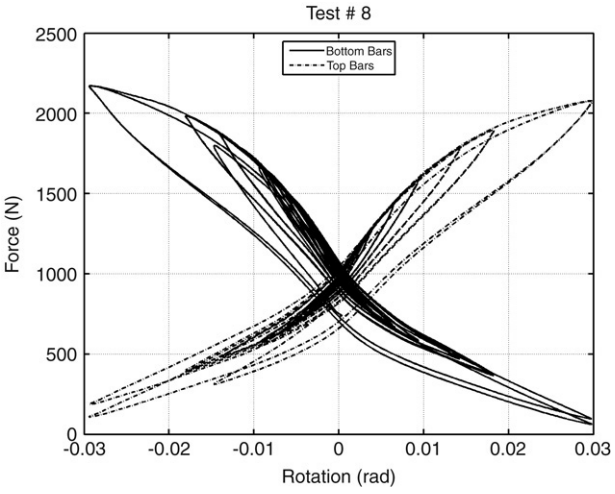

Fig. 11. Top and bottom bar forces as a function of equivalent joint rotation.

5.5%. During the different tests, the rods were subjected to a maximum strain of 1.7%.

Fig. 14 shows the average of the energy loss per cycle for a test performed at 0.25 Hz, calculated from the hysteresis loops of each rod and from the complete assembly. Most of the energy is effectively dissipated by the rods.

After 216 cycles no sign of deterioration was noted in any rod and residual strains at the SMA bars were negligible.

4. Dynamic analysis of a three-story frame

In order to compare the dynamic performance of a rigid steel frame and a partially restrained frame with SMA connections, a three-story benchmark structure was selected for preliminary numerical analysis using the nonlinear analysis program DRAIN-2DX [15]. Fig. 15 shows an elevation of the frame model with SMA connections. Spans were all 9.14 m and story heights were 3.96 m. The structures were considered fixed at the base. Floor masses and member sizes are listed in Table 2. Yield stresses for beams and columns were 350 and 404 MPa, respectively.

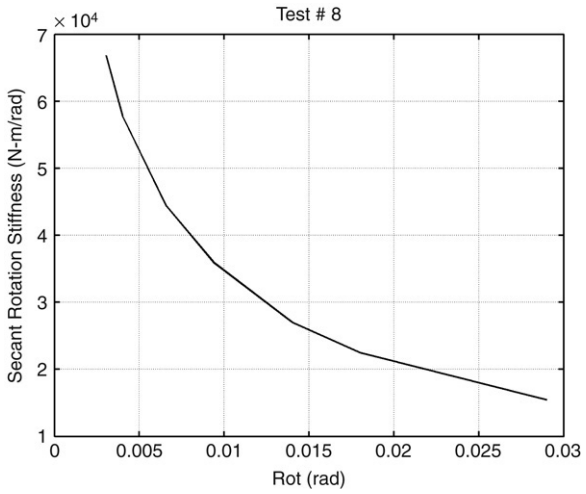

Fig. 12. Secant rotation stiffness as a function of maximum cyclic rotation.

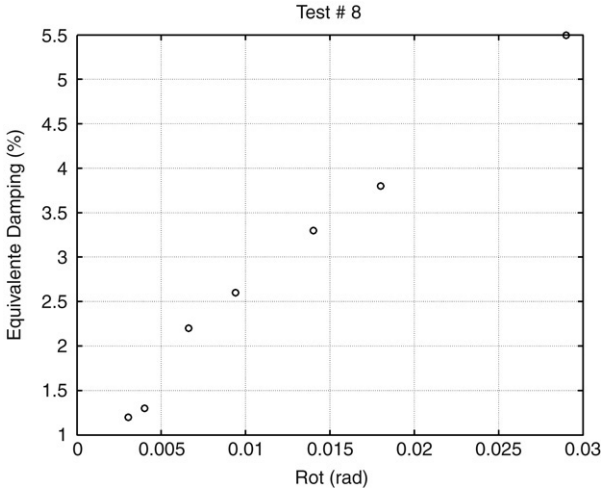

Fig. 13. Equivalent critical damping ratio as a function of maximum cyclic rotation.

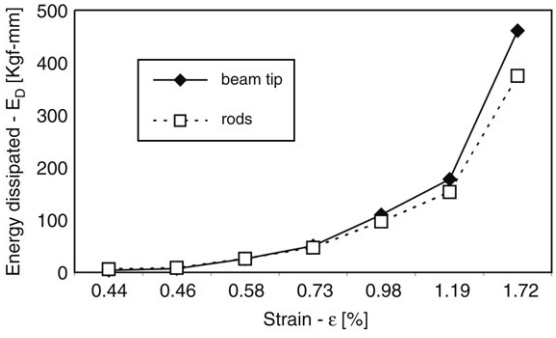

Fig. 14. Energy dissipated by the rods and the connection.

Table 2
Masses and member sizes

Story	Masses N ∗ sec^2/cm	Columns exterior	interior	Girder
1	4915	W14 × 257	W14 × 311	W30 × 116
2	4915	W14 × 257	W14 × 311	W30 × 116
3	5318	W14 × 257	W14 × 311	W24 × 62

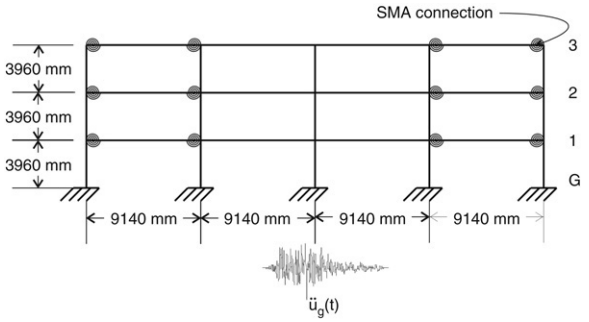

Fig. 15. Elevation of three-story frame model.

Each SMA connection element consisted of a bundled group of 3 mm diameter wires that were assumed to be placed above the top flange and below the bottom flange of the beams. By varying the number of wires and/or the initial elastic modulus, the natural period of the SMA connected frame varied between 0.92–1.15 sec while the natural period of the rigid frame was 0.91 sec. Two earthquake records were considered in the simulations: Rinaldi 228 (1994, peak acceleration = 0.82 g) and Llolleo N10E (1985, peak acceleration = 0.65 g). Mass and stiffness proportional Rayleigh damping was used, with an equivalent viscous damping ratio of 2% for modes 1 and 3.

A beam–column element with plasticity concentrated at its ends (Element 2 in DRAIN-2DX) was used to model beams and columns, and an inelastic rotational spring element (Element 4 in DRAIN-2DX) was used to model the SMA connection. The properties of the inelastic rotational spring were determined assuming a Young Modulus variation between 70 GPa (from static test) to 1.2 GPa (from dynamic test). A hardening ratio between 0.17 and 0.4 was considered. In most cases, a total area of SMA wires of 28 cm^2 per bundle was considered with a length of 18.2 cm. Yielding moment varied between 5.7 and 33.3 kN m and the initial stiffness varied from 9.13 to 532 MN m/rad.

In order to examine the overall response of the structures, the story displacements, story drifts, residual drifts, and story shears were determined. The following conclusions yield from the comparison of the above parameters:

- For the Llolleo record although story shear diminishes by 10%, displacements and drifts are about the same than in the rigid frame. The maximum rotation was 0.022 rad which corresponds to an axial strain of 4.2%. This value is larger than the superelastic limit of the material.
- For Rinaldi 228-story shear, displacement and drifts are slightly reduced but the maximum rotation was up to 0.06 rad, meaning an axial strain of 11.5%, which is largest than the fracture limit. Probably with a larger rod some improvement could be attained.
- In all cases the steel elements are dissipating much energy than the SMA connections.

5. Conclusions

Shape memory alloys exhibiting superelastic effect possess characteristics that make them ideal for applications in passive control of seismic response of buildings. Innovative steel

connections with SMA copper-based rods were evaluated. In order to verify the superelastic effect, isolated rods were subjected to static monotonic and dynamic cyclic tests.

Several thermal treatments were evaluated to obtain an appropriate grain size. Final energy dissipation and deformation capacities are highly dependent on this treatment. Appropriate treatment of bars is difficult to attain because of its dependence on material composition and specimen size.

The SMA response is also highly dependent on the pre-tension stress, so this parameter shall be carefully controlled. In the test arrangement, gravity loads imposed a difficult condition and limited the possibility of having a symmetrical response.

Stable cycles for deformations were obtained with the appropriate thermal treatment and training of the bars. Rotations up to 0.03 rad were obtained without any damage or residual displacements, and hysteretic loops were quite stable and repeatable. Secant stiffness and energy dissipation capacity of the joint is highly dependent on bar deformation. Equivalent damping ratios up to 6% were obtained on tests of individual bars subjected to strains up to 2.6%, while values up to 5.5% were observed in the beam–column assembly, where the bars reached strains up to 1.7%.

Preliminary numerical simulations indicate that the inclusion of CuAlBe rods at the beam–column connections does not improve the response of a structure to seismic load due to the fact that the SMA connections are more flexible than the rigid ones and, therefore, can actually increase the displacement response of the structure for ground motions. However, more analysis results with different frame configurations need to be studied before a definitive conclusion can be stated regarding the advantages of using SMA connections in moment-resisting frames.

Acknowledgements

The authors gratefully acknowledge that this research was financially supported by the University of Chile and Fondecyt projects No 1030554 and No 1070370.

References

[1] AISC. Seismic provisions for structural steel buildings. Chicago (IL): American Institute of Steel Construction; 2005.

[2] Bernardini D, Brancaleoni F. Shape memory alloys modeling for seismic applications, In: Proceedings of the MANSIDE final workshop. Rome (Italy): Servizio Sismico Nazionale; 1999. p. II73–84.

[3] Bruneau M, Engelhardt M, Filiatrault A, Goel S, Itani A, Hajjar J, et al. Review of selected recent research on US seismic design and retrofit strategies for steel structures. Progress in Structural Engineering and Materials 2005;7(3):103–14.

[4] Cardone D, Dolce M, Ponzo FC, Coelho E. Experimental behaviour of R/C frames retrofitted with dissipating and re-centering braces. Journal of Earthquake Engineering 2004;8(3):361–96.

[5] Casciati F, Faravelli L. Experimental characterization of a Cu-based shape memory alloy toward its exploitation in passive control devices. Journal de Physique IV 2004;115:299–306.

[6] DesRoches R, Smith B. Shape memory alloys in seismic resistant design and retrofit: A critical review of their potential and limitations. Journal of Earthquake Engineering 2004;8(3):415–29.

[7] DesRoches R, McCormick J, Delemont M. Cyclic properties of superelastic shape memory alloy wires and bars. Journal of Structural Engineering 2004;130(1):38–46.

[8] Dolce M, Cardone D. Mechanical behavior of shape memory alloys for seismic application 1. Martensite and austenite NiTi bars subjected to torsion. International Journal of Mechanical Sciences 2001;43(11): 2631–56.

[9] Dolce M, Cardone D. Mechanical behavior of shape memory alloys for seismic application 2: Austenitic NiTi wires subjected to tension. International Journal of Mechanical Sciences 2001;43(11):2657–77.

[10] Dolce M, Cardone D, Ponzo FC, Valente C. Shaking table tests on reinforced concrete frames without and with passive control systems. Earthquake Engineering and Structural Dynamics 2005;34(14):1687–717.

[11] FEMA. Recommended seismic design criteria for new steel moment-frame buildings. Report no. FEMA 350. Washington (DC, USA): Federal emergency management agency; 2000.

[12] Flores-Zúñiga H, Ríos-Jara D, Belkahla S, Nika V, Guénin G. The training and re-training procedures for the two way memory effect and its degradation in a Cu–Al–Be alloy. Scripta Materialia 1996;34(12): 1899–904.

[13] Gillet Y, Patoor E, Berveiller M. Beam theory applied to shape memory alloys. In: A. Pelton, D. Hodgson, and T. Duerig, editors. Proceedings of the first international conference on shape memory and superelastic technologies, 1994. p. 169–74.

[14] Ocel J, DesRoches R, Leon RT, Hess WG, Krumme R, Hayes JR, Sweeney S. Steel beam–column connections using shape memory alloys. ASCE Journal of Structural Engineering 2004;130(5):732–40.

[15] Prakash V, Powell GH, Filippou FC. DRAIN-2DX: Base program user guide. Report No. UCB/SEMM-92/29. University of California at Berkeley; 1992.

[16] Priestley MJN. Overview of presss research program. PCI Journal 1991; 36(4):50–7.

[17] Song G, Ma N, Li H. Applications of shape memory alloys in civil structures. Engineering Structures 2006;28(9):1266–74.

[18] Torra V, Isalgue A, Martorell F, Terriault P, Lovey F. From experimental data to quake damping by SMA: A critical experimental analysis and simulation. In: Proc. 9th World seminar on seismic isolation, energy dissipation and active vibration control of structures. 2005.

[19] Wilson JC, Wesolowsky MJ. Shape memory alloys for seismic response modification: A state-of-the art review. Earthquake Spectra 2005;21(2): 569–601.

[20] Witting PR, Cozzarelli FA. Shape memory structural dampers: Materials properties, design and seismic testing. Technical report MCEER 92-0013. Buffalo (NY): State University of New York; 1992.